An efficient method to improve the spatial resolution of laboratory X-ray diffraction contrast tomography

Paper

Fang, H.; Juul Jensen, D.; Zhang, Y.

Published in:
I O P Conference Series: Materials Science and Engineering

Link to article, DOI:
10.1088/1757-899x/580/1/012030

Publication date:
2019

Document Version
Publisher's PDF, also known as Version of record

An efficient method to improve the spatial resolution of laboratory X-ray diffraction contrast tomography

IOP Conf. Series: Materials Science and Engineering **580** (2019) 012030 doi:10.1088/1757-899X/580/1/012030

An efficient method to improve the spatial resolution of laboratory X-ray diffraction contrast tomography

H Fang[1], D Juul Jensen[1] and Y Zhang[1]

[1]Department of Mechanical Engineering, Technical University of Denmark, 2800 Kgs. Lyngby, Denmark.

E-mail: hfang@mek.dtu.dk

Abstract. Lab-based diffraction contrast tomography (LabDCT) has recently enabled non-destructive 3D characterization of the crystallographic orientations and grain morphologies in bulk materials. Despite the wide accessibility and availability of lab-based X-rays, the current spatial resolution of LabDCT is only about 20 μm and has to be improved to make this technique a more versatile tool. Conventional LabDCT takes advantage of the Laue focusing effect, *i.e.* the diffracted beam from a sample illuminated by an incoming polychromatic beam, is focused when the source and the detector are symmetrically positioned. In this study we have investigated the possibility of increasing the spatial resolution of LabDCT by placing the detector at a distance beyond that required for Laue focusing. We first developed a forward projection simulation tool to elucidate the effects of placing the detector at a larger distance. Next, we performed LabDCT measurements on a partially recrystallized pure aluminum sample at different sample-to-detector distances. The results show that the diffraction spots can be magnified by a factor of about three compared to the current LabDCT setup. The benefits and limitations resulting from increasing the sample-to-detector distance are discussed.

1. Introduction

The properties of most polycrystalline materials, such as metals and ceramics, depend to a large extent on the size, shape and crystallographic orientation of the crystalline grains that constitute such materials. At present, the most widely used technique to characterize grain shapes and orientations is electron backscatter diffraction (EBSD) [1, 2]. However, the electrons limit the characterization to only 2D and requires a destruction of the sample when combined with serial sectioning to achieve mapping in 3D. Recently, 3D mapping of grain orientations with a resolution down to 1 nm using transmission electron microscopy (TEM) has been demonstrated on an aluminum sample with a thickness of about 150 nm [3]. Despite the high resolution of this technique, the probed sample volume is restricted to the nanometer regime. To enable non-destructive characterization of grain structures in 3D for polycrystalline materials at the micron and submicron length scales, several techniques at synchrotron radiation sources have been developed over the past two decades. The main examples of these techniques are differential aperture X-ray microscopy (DAXM) [4], three-dimensional X-ray diffraction microscopy (3DXRD) [5] and diffraction contrast tomography (DCT) [6]. Although all these techniques are very useful for determination of the grain structure in 3D, they require an intense X-ray beam that is available only at synchrotron radiation sources. This restriction places a serious limit in accessibility for a wide range of experiments, *e.g.* when many repeated measurements, or very time consuming ones, are needed.

A transition to the use of a laboratory X-ray source for DCT has been recently made. It has been demonstrated that lab-based diffraction contrast tomography (LabDCT) is able to determine non-destructively the size, position, shape and orientation of grains in 3D [7, 8]. In the current LabDCT set-up, the sample and the detector are placed such that the sample-to-source distance L_{ss} equals the sample-to-detector distance L_{sd}, which focuses the diffracted pattern of the grains into lines on the detector. This so-called Laue focusing does not provide any geometrical magnification of the diffraction spots. The current spatial resolution that can be achieved with this set-up is rather limited (about 20 μm), which has to be improved to make LabDCT a more versatile tool for studying a wide range of materials science problems.

In the current work, we explore the potential for improving the resolution of LabDCT by increasing the ratio of L_{sd}/L_{ss}, thereby geometrically magnifying the diffraction spots. To achieve this aim, we first develop a computational tool to simulate forward projections of an already-known 3D grain structure and investigate the effect of L_{sd}/L_{ss} on features of the diffraction spots to verify our ideas. Then the diffraction projections of a partially recrystallized pure aluminum sample are measured using LabDCT at different ratios of L_{sd}/L_{ss}. The resulting diffraction spots for the same grains are compared for different L_{sd}/L_{ss} and validated by the forward simulations. The effect of increasing L_{sd}/L_{ss} on the geometrical magnification is also evaluated and demonstrated to be promising for increasing the resolution. The benefits and limitations by increasing the ratio of L_{sd}/L_{ss} are also discussed.

2. Simulations of forward projections

Methods for computation of forward projections for synchrotron 3DXRD and for the variant synchrotron DCT, where both use a parallel and monochromatic beam, have been described elsewhere [5, 9, 10]. However, the LabDCT is characterized by use of a cone-shaped polychromatic X-ray beam. This means that the formation of forward projections in LabDCT has some distinct features differing from those of synchrotron DCT. Here we briefly describe our simulations of the forward projections for LabDCT.

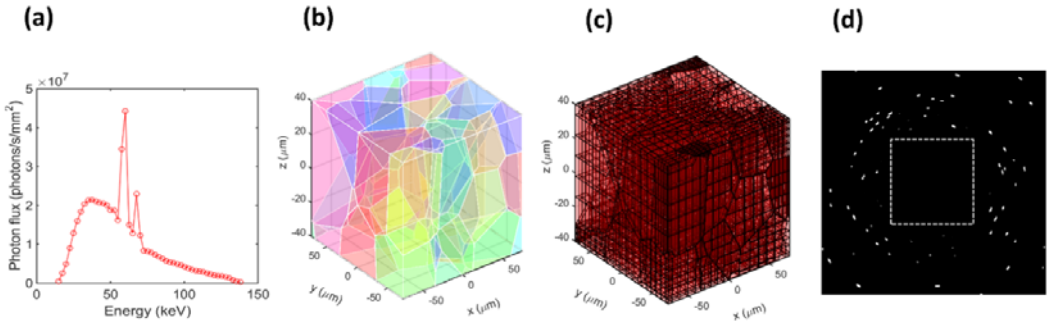

Figure 1. Illustration of the workflow of the forward simulations of projections for a sample with known grain morphologies and orientations in 3D. (a) Spectrum of the laboratory X-ray source using a tungsten target; (b) 3D visualization of a virtual alpha iron sample of a rectangular shape ($L_x \times L_y \times L_z = 150 \times 150 \times 80$ μm^3); (c) polyhedral mesh of the sample, and (d) simulated projection at a rotation angle $\omega = 0^o$ and $L_{ss} = L_{sd} = 14.0$ mm with the edge of beam-stop marked by the dashed line.

The laboratory X-ray source is assumed to be a point as the X-ray beam is usually focused to a size of about 4 μm that is negligible compared to L_{ss} and L_{sd}. The profile of the X-ray spectrum emitted from a tungsten target is shown in figure 1a. Figure 1b shows a virtual polycrystalline alpha iron sample with randomly generated grain orientations that is used as here as the input. The simulations can also be carried out using 3D maps of grains from any available data source as an input. The virtual sample is then discretized into polyhedral cells in 3D, shown in figure 1c, to accelerate the computation. In this way we can determine the position, shape and intensity of diffraction spots from each polyhedral. By collecting the diffraction spots for all polyhedral cells, one can derive projection images at any rotation

angle ω. An example is shown in figure 1d. The current simulations were performed using MATLAB® and the projections were exported in the form of 16-bit grey images.

3. Experimental

A partially recrystallized pure aluminium (99.996 wt.% Al) sample was selected to demonstrate the magnification of diffraction spots by increasing L_{sd}/L_{ss} in the LabDCT set-up. A rectangular sample ($6.0 \times 4.0 \times 1.3$ mm^3) was cut from a 12% cold-rolled pure Al plate and electro-polished. An Vickers hardness indent was made on the plane defined by the rolling direction (RD) and transverse direction (TD) to stimulate formation of nuclei upon annealing. More detailed descriptions of how the indentation was made can be found elsewhere [11]. The sample was then annealed at temperatures in the range from 275 °C to 340 °C for a total time of 50 min. After annealing the deformed structure is partially recrystallized and new grains with an average grain size of about 100 μm are found adjacent to the indentation site. This partially recrystallized sample was characterized by LabDCT.

Table 1. Values of L_{ss} and L_{sd} for LabDCT measurements of the partially recrystallized Al sample

Scan	L_{ss} (mm)	L_{sd} (mm)	L_{sd} / L_{ss}
I	14.0	14.0	1.00
II	11.0	18.0	1.64
III	11.0	24.0	2.18

The LabDCT measurements were performed on a Zeiss Xradia 520 Versa X-ray microscope. A detector (2032×2032) with an effective pixel size of 3.36 μm was used for recording the diffraction patterns. Three different ratios of L_{ss} and L_{sd} were used, as listed in table 1. The exposure time for each projection was 600 s. For reconstruction of the grains in 3D, the sample was rotated through 360° with a step of 2° during the scan. The GrainMapper3D™ software was used for indexing and mapping of grains from the LabDCT projections. ParaView was employed to visualize the grain structure.

4. Results and discussion

4.1. Simulations of forward projections

Figure 2 shows simulated forward projections at two different ratios of L_{sd}/L_{ss} and a rotation angle of 30° for the virtual alpha iron sample with the grain structure shown in figure 1b. By increasing L_{sd}/L_{ss} from 1 to 1.64, the diffraction spots formed for lattice planes of the same grain are geometrically magnified. For example, the 002 diffraction spot of grain 32 (grain diameter = 61.9 μm) is magnified by a factor of 1.91, while a magnification of 1.76 is found for the $11\bar{2}$ spot of grain 17 (grain diameter = 56.7 μm). This magnification is not symmetric. The diffractions spots are magnified more in the radial direction (a factor of about 1.6) than in the azimuthal direction (a factor of about 1.2) as L_{sd}/L_{ss} is increased from 1 to 1.64.

The field of view (FOV) captured in the projection is reduced by increasing L_{sd}/L_{ss}, as is clearly seen in figure 2. This is because the accessible maximum scattering angle $2\theta_{max}$ is decreased. However, some diffraction spots blocked by the beam-stop at $L_{sd}/L_{ss} = 1$ can be seen at $L_{sd}/L_{ss} = 1.64$. Examples of these diffraction spots are the $0\bar{1}\bar{1}$ spot of grain 3 (grain diameter = 29.1 μm^3) and the 200 spot of grain 30 (grain diameter = 29.6 μm) marked by triangles in figure 2b. This demonstrates that although increasing L_{sd}/L_{ss} results in a reduced FOV it also increases the likelihood to obtain diffraction signal from smaller 2θ angles on the detector.

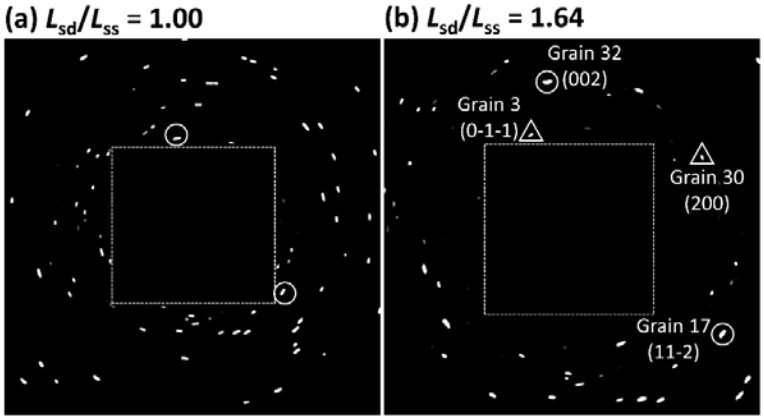

Figure 2. Simulated forward projections at $\omega = 30^{o}$ of a virtual alpha iron sample consisting of 48 grains with an average diameter of 35 μm and randomly generated orientations for different L_{sd}/L_{ss} ratios. (a) L_{ss} and L_{sd} = 14.0 mm; (b) L_{ss} = 14.0 mm and L_{sd} = 22.9 mm. Circles mark the diffraction spots seen on both images while triangles mark the diffraction spots seen only in (b). The grain identification number and Miller indices of the marked spots are also shown. The edges of the beam-stop are marked by dashed lines.

4.2. LabDCT measurements at different values of L_{sd}/L_{ss}

Figure 3 shows the 3D grain structure reconstructed from LabDCT measurement at $L_{ss} = L_{sd}$ = 14.0 mm. All the grains except grain 2 are recrystallized. Grain 2 is only recovered and has an internal substructure with a spread of orientations. For convenience we use at present the average orientation Euler angles to represent this grain as an input for forward simulation.

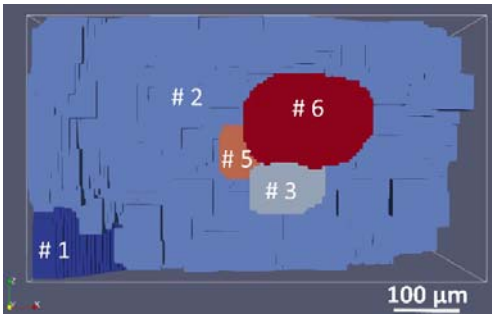

Figure 3. A front view of the 3D grain map reconstructed from the LabDCT measurement at L_{ss} = L_{sd} = 14.0 mm. The grain numbers are marked. Grain 4 is not seen because it is located behind the junctions of grains 3, 5 and 6. Random colors are used.

Figure 4 compares the projections of diffraction patterns at a rotation angle of ω = -146° from both the LabDCT measurements and forward simulations for L_{sd}/L_{ss} = 1.00, 1.64 and 2.18 using an input sample shown in figure 3. At this rotation angle diffraction spots for all grains in the sample can be found. Comparing figures 4a with 4b, it is seen that the common diffraction spots are significantly magnified as L_{sd}/L_{ss} is increased to 1.64, as also shown in the forward simulations in figures 4d and 4e. For L_{sd}/L_{ss} = 2.18 the diffraction spots shown in projection for L_{sd}/L_{ss} = 1.00 are mostly missing, except the four diffraction spots, $\bar{1}1\bar{3}$ of grain 6, $\bar{1}1\bar{3}$ and $1\bar{3}\bar{1}$ of grain 2 and $1\bar{1}1$ of grain 5, which are partially present and significantly magnified (see figures 4c and 4f). It can also be seen that new diffraction spots are seen on the detector, such as the $\bar{2}20$ spot of grain 1. The magnifications on average are about 2.4 at L_{sd}/L_{ss} = 1.64 and 3.5 at L_{sd}/L_{ss} = 2.18.

Figure 4 also shows that the positions and shapes of the simulated diffraction spots for the recrystallized grains are in very good agreement with the measurements. However, in figure 4a some

relatively large diffraction spots, marked by circles, do not appear in figure 4d. Since the forward simulations uses inputs from the reconstructed grain structure, the simulated projection should ideally be identical to the measured one. These missing spots in the simulation suggest that one or more grains have not been indexed during reconstruction using the GrainMapper^{TM} software. The shapes of the diffraction spots for grain 2 are also different. In the LabDCT measurements the diffraction spots from grain 2 are much larger and more blurred than those shown in the simulated projections. This can be understood though as only the average orientation was used for grain 2 in the simulations, whereas this grain is in fact a recovered deformed grain and has significant variation in interior orientations. The comparison between the simulated and the measured projections demonstrates nevertheless that the present forward simulation is a very useful tool for evaluating the reconstruction results.

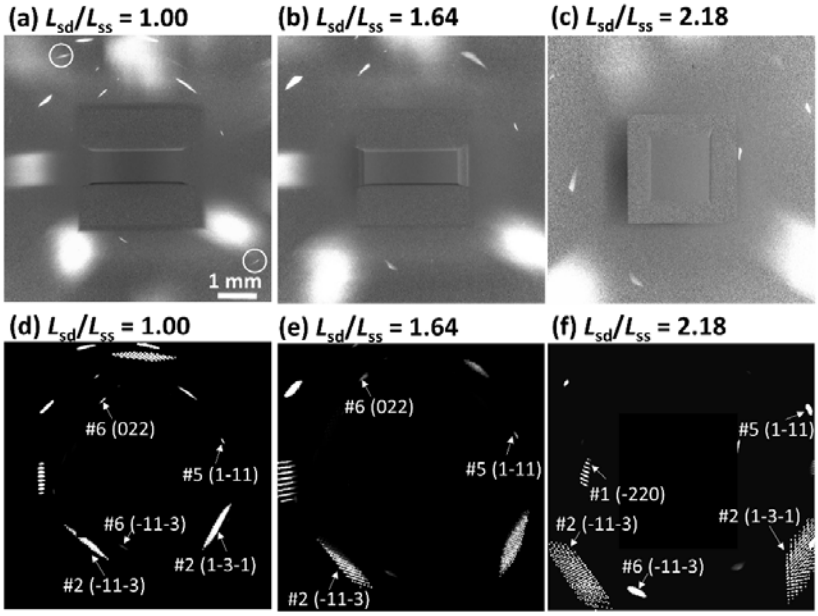

Figure 4. Projections of diffraction patterns rendered by LabDCT measurements (a, b and c) and from forward simulations (d, e and f) for L_{sd}/L_{ss} = 1.00, 1.64 and 2.18. The scale bar shown in (a) applies to all projections. Missing spots in the simulations are marked by circles in (a). Indices of the diffraction spots are shown in the simulated projections. The edges of the beam-stop are not shown in the simulated projections for clarity.

4.3. Discussion

4.3.1. Benefits of increasing L_{sd}/L_{ss}. A geometrical magnification is demonstrated by the projections from both the experimental LabDCT measurements and from the forward simulations. In total, we compared the size of 97 diffraction spots for different rotation angles at L_{sd}/L_{ss} = 1 and 1.64. The results show that the spot size is magnified by a factor between 1.2 and 9.0 depending on the diffraction planes and volumes of the grains. On average a value of 2.2 is found. Further increase of L_{sd}/L_{ss} enhances this magnification. However, such an increase also results in a lack of sufficient statistics for the diffraction spots, as most diffraction spots recorded at L_{sd}/L_{ss} = 1 cannot be captured when L_{sd}/L_{ss} > 2. A detector with a larger area would be needed for such analysis using larger values of L_{sd}/L_{ss}. Nonetheless, figure 4 indicates that a magnification factor of about 3.5 can be reached when L_{sd}/L_{ss} is close to 2.18. It is also necessary to evaluate how such a magnification affects the quality of the magnified diffraction spots, including sharpness and blurring, which should not be compromised to ensure a proper grain mapping. To evaluate the sharpness, we compared the full width half maximum (FWHM) of the derivative of the

histogram profile across the edges of diffraction spots from LabDCT for the three scan conditions (I, II and III in table 1). We found that the FWHM values are almost equal for the three ratios of L_{sd}/L_{ss}. The variations of grey values for each diffraction spot are also calculated to evaluate the blurring. The values fluctuate around 0.05 ± 0.02 as a function of spot size and no significant difference is found as L_{sd}/L_{ss} is increased. Therefore, it is concluded that increasing L_{sd}/L_{ss} does not compromise the quality of the diffraction spots, demonstrating that increasing L_{sd}/L_{ss} can be an efficient method to improve the spatial resolution for LabDCT.

4.3.2. Limitations of increasing L_{sd}/L_{ss}. The maximum accessible scattering angle $2\theta_{max}$ decreases from about 19° to 9° as L_{sd}/L_{ss} is increased from 1 to 2.73, assuming a fixed detector size. This imposes an upper limit for increasing L_{sd}/L_{ss}. According to our simulations, $2\theta_{max}$ should be larger than 10° to ensure a sufficient number of pronounced diffraction spots that can be easily segmented from the background noise. Therefore, with the present detector L_{sd}/L_{ss} should be in the range 1.50 ~ 2.45 to achieve at the same time both a considerable magnification and a satisfactory number of diffraction spots. Of course this limitation can be overcome by using a detector with a larger recording area.

5. Conclusions

In this study we have investigated the possibility of increasing L_{sd}/L_{ss} as a method to improve the spatial resolution of LabDCT. A forward simulation tool has been developed and applied to simulate LabDCT projections of a virtual sample and a real sample. The forward simulations show that increasing L_{sd}/L_{ss} is very effective in achieving a geometrical magnification of diffraction spots. Experimental LabDCT measurements confirm this result and show that the image quality is compromised as L_{sd}/L_{ss} is increased. Magnification factors of between 2 and 3.5 are found for $1.64 < L_{sd}/L_{ss} < 2.18$ compared to that under the Laue focusing condition $L_{sd}/L_{ss} = 1$. The agreement and disagreement between the simulated diffraction patterns and experimental LabDCT measurements both provide further insights into 3D grain mapping with more fine details. The present study demonstrates that increasing L_{sd}/L_{ss} can be an efficient method for improving the spatial resolution for the LabDCT.

Acknowledgements

The authors thank the financial support by the European Research Council (ERC) under the European Union's Horizon 2020 research and innovation programme (M4D – grant agreement No. 788567).

References

[1] Venables J A and Harland C J 1973 *Philos. Mag.* **27** 1193
[2] Krieger Lassen N C, Juul Jensen D and Conradsen K 1994 *Acta Cryst.* **A50** 741
[3] Liu H H, Schmidt S, Poulsen H F, Godfrey A, Liu Z Q, Sharon J A and Huang X 2011 *Science* **332** 833
[4] Larson B C, Yang W, Ice G E, Budai J D and Tischler J Z 2002 *Nature* **415** 887
[5] Poulsen H F 2004 *Three-dimensional X-ray diffraction microscopy: mapping polycrystals and their dynamics*. Springer Tracts in Modern Physics vol. 205. (Berlin: Springer) p 25
[6] Ludwig W, Schmidt S, Lauridsen E M and Poulsen H F 2008 *J. Appl. Cryst.* **41** 302
[7] King A, Reischig P, Adrien J and Ludwig W 2013 *J. Appl. Cryst.* **46** 1734
[8] Sun J, Zhang Y, Lyckegaard A, Bachmann F, Lauridsen E M and Juul Jensen D 2019 *Scrip. Mater.* **163** 77
[9] Oddershede J, Schmidt S, Poulsen H F, Sorensen H O, Wright J and Reimers W 2010 *J. Appl. Cryst.* **43** 539
[10] Sørensen H O, Schmidt S, Wright J P, Vaughan G, Techert S, Garman E F, Oddershede J, Davvasambu J, Paithankar K S, Gundlach C and Poulsen H F 2012 *Zeitschrift für Kristallographie Cryst. Mater.* **227** 63
[11] Xu C, Zhang Y, Godfrey A W, Wu G, Liu W, Tischler J Z, Liu Q and Juul Jensen D 2017 *Sci. Rep.* **7** 42508